International Journal of Advanced Multidisciplinary Application | IJAMA
Volume 3 Issue 11 Nov 2026
ISSN No: 3048-9350

Preparation And Characterization Of Metallated Carbon Black From Turmeric Spent

Saigeetha V S[1] Rajesh C [2] George Mathew[1*]
[1]Research scholar, St. Mary's College, PG and Research Department of Chemistry, University of Calicut, Sulthan Bathery, Kerala, India.
[2]Associate Professor, [2]MES Keveeyam College, University of Calicut, Valanchery, India.
[1*]Assistant Professor, St. Mary's College, PG and Research Department of Chemistry, University of Calicut, Sulthan Bathery, Kerala, India.
Emai: [1]saimalu999@gmail.com,[2] rajeshchem77@gmail.com,[3]gmathew7@gmail.com

Abstract

Turmeric spent refers to the residual material left after extracting curcumin and other bioactive compounds from turmeric rhizomes, which is utilized as a precursor for preparing carbon black and metalated carbon black. Carbon black received from turmeric spent is modified with Zn, Ni, Pb and Fe ions to investigate the influence of metal incorporation on its physicochemical properties. Atomic absorption spectroscopy (AAS) confirmed the presence of the respective metals in carbon black derived from spent turmeric. Elemental composition of each sample is analysed using CHNS analysis. Scanning electron microscope with energy dispersive X-ray spectroscopy (SEM-EDS) was used to confirm the presence of corresponding metals in carbon black. Nickel presence was confirmed using AAS even though it was masked in SEM EDS. Particle size distribution was analysed using Dynamic light scattering (DLS) and showed that L_1 exhibited the smallest diameter of 35.9nm compared to other samples. The metalated samples exhibited less negative zeta potentials than CS (−11.9 mV), indicating surface-charge neutralization and reduced colloidal stability following metal adsorption. X-ray diffraction analysis (XRD) confirmed the formation of characteristic crystalline phases associated with Fe_3O_4, Fe_2O_3, PbO/lead-containing phases, ZnO/Zn, and Ni/NiO, depending on the metal treatment. The overall study showed that turmeric spent can serve as a low-cost potential biomass precursor for the preparation of metalated carbon black with tunable structural, surface and electrical properties, offering potential for applications in adsorption, catalysis, electrochemical systems and other value-added technologies.

Keywords: *Metalated carbon black. Lead loaded carbon black. zinc loaded carbon black. Iron loaded carbon black, Nickel loaded carbon black*

1.INTRODUCTION

Curcumin (Slaček et al., 2023) extracted from turmeric(Goel et al., 2008) is well known for its health benefits and medicinal properties, resulting from its antioxidant, antiseptic, wound healing and anti-inflammatory effects. The applications (Landim Neves et al., 2020) extend over a wide spectrum via a condiment, flavour enhancer, food additive, food preservative and as a special additive in Ayurvedic, Yunani and Sidha medicines (Joshi et al., 2021) Curcumin also owns its place. "Turmeric spent" refers to the residual material left after extracting curcumin and other bioactive compounds from turmeric rhizomes(Cakrawati et al., 2024). This by-product, often considered waste, has gained attention for its potential applications

across various industries. This is due to its rich content of dietary fiber, antioxidants, and other bioactive compounds(Nampoothiri et al., 2012). Owing to its high fiber content, turmeric spent is increasingly incorporated into livestock and poultry feed to promote digestive health and provide essential nutrients. The dietary fibre in turmeric spent has been linked to several health benefits, including enhanced gut health and potential anti-obesity effects. Research suggests that the inclusion of turmeric spent in diets can lead to reduced fat mass in rats subjected to high-fat feeding as a result of its indigestible carbohydrates and fermentative potential in the gut (Nampoothiri et al., 2012). Studies have shown that enriched spent turmeric oleoresin (STO) exhibits significant antioxidant activity and contains higher concentrations of curcuminoids than the original STO. These properties suggest potential uses in food preservation and as a natural colorant (Nagarajan et al., 2010). Apart from its various health-related applications, turmeric spent has been proven to be an effective additive for polymers.

Turmeric spent has been explored as a filler in unsaturated polyester composites, enhancing properties like tensile strength and chemical resistance, making it suitable for eco-friendly material applications(Syed et al., 2010). Using appropriate chemical treatments, turmeric spent can be converted into nanofibers with antimicrobial and antioxidant properties, opening avenues for use in pharmaceuticals and bio composites(Nampoothiri et al., 2012). Turmeric essential oil, blended with pectin and sodium alginate, poly lactic acid polymers, was used as a sustainable food packaging material. It adds functional properties such as UV-blocking and provides antibacterial action against *E. coli* and *S. aureus*, helping to extend food shelf life(Bužarovska et al., 2025) (Shambu et al., 2026).Turmeric bulbs can serve as a substitute for coarse aggregate in geopolymer concrete, with optimal performance achieved at up to 30% replacement for sustainable construction materials.(Kanagaraj et al., 2024).

The rapid growth of urbanization and industrialization has put pressure on water resources, hindering the sustainable development of societies and economies(Z. Wang et al., 2022)(Zha et al., 2021)(Luo, P., Mu, Y., Wang, 2022). Water pollution, climate change, and intensive human activities have a profound effect on watersheds(Z. Wang et al., 2022)(Lu & Yu, 2018)(Mu et al., 2021)(Zhu et al., 2022)(Luo et al., 2022). Human activities such as agriculture, mining, industrial processes, and urbanization contribute to the release of significant amounts of heavy metals into aquatic environments. Recent studies emphasize that heavy metal contamination in water has become a major global environmental concern. This issue is largely fueled by the expansion of mining and refining operations and the manufacture of metal-containing products.

Heavy metal (HM) pollution occurs when the concentrations of HMs and their compounds in water exceed allowable limits, thereby preventing natural self-purification. Heavy metals present in wastewater, particularly those from metal plating, electroplating, steel, mining industries, and battery manufacturing, production of printed circuit boards (PCBs), wood processing, petroleum refining, textile and tannery industry operations, represent a major threat to both environmental and human health (Wei et al., 2018)(Hamdy et al., 2019)(Sharma et al., 2022)(R. Wang et al., 2021)(Narayan Thorat & Kumar Sonwani, 2022)(Nur-E-Alam et al., 2020). Many HMs possess carcinogenic, teratogenic, mutagenic, non-biodegradable, and bioaccumulative properties. When these metals enter the human body through various routes, they can cause symptoms ranging from mild issues like headaches and joint pain to more severe conditions such as mental disorders, abnormal liver and kidney

function, and even cancer(Klaudia Jomova , Suliman Y Alomar , Eugenie Nepovimova , Kamil Kuca, 2025)(Dasharathy et al., 2022). Trace elements such as arsenic (As), cadmium (Cd), chromium (Cr), cobalt (Co), copper (Cu), lead (Pb), mercury (Hg), nickel (Ni), and zinc (Zn) are recognized as metallic pollutants in wastewater, industrial effluent, and sewage sludge(Staszak & Wieszczycka, 2023)(Shahabi Nejad & Sheibani, 2022)(Qasem et al., 2021)(Kerur et al., 2020). The World Health Organization has established maximum contaminant or permissible limits for As, Cu, Pb, Cd, Cr, Co, Hg, Ni, and Zn in drinking water at 0.01, 2.5, 0.05, 0.003, 0.05, 0.1, 0.001, 2.0, and 5.0 mg/L, respectively (Karim et al., 2023). In freshwater, iron can be found in a concentration of 0.5-5mg/L and considering these factors, the World Health Organization (WHO) restricts the iron level in drinking water to 0.3 mg/L (World Health Organization, 2004). Although iron is an essential element for human health, excessive concentrations cause a wide range of health problems, such as cognitive disorders (Anbari et al., 2017) and hemochromatosis, which can damage different organs of the body(Khatri et al., 2017). Iron is considered a secondary contaminant because it is not harmful to humans but can cause aesthetic issues such as taste issues, turbidity, and discoloration (Hashim et al., 2017). Lead (Pb) is the second most toxic metal, making up 0.002% of the Earth's crust. It is naturally present in very small quantities but is primarily produced by human activities such as industry, automobiles, and batteries. As a result, lead pollution is impacting both humans and the environment. Many of the Pb salts/oxides originate from dust, battery vents, lead paint, and contaminated diet, which is the major route of human exposure(Raj & Das, 2023)(Tripathy, Banismita, Akankshya, 2024) . Especially, canned food industries are a main cause of lead consumption due to the leaching characteristics in canned foods(Raj & Das, 2023). Lead exposure can have serious health implications, especially for children, including developmental delays, learning difficulties, and behavioural problems. In adults, prolonged exposure can lead to high blood pressure, kidney damage, and reproductive issues (WHO, (2023). Zinc is an essential element for the proper functioning of the body, but in excess it can cause several health issues. Prolonged exposure to high levels of zinc can cause immune dysfunction, reduced high-density lipoprotein (HDL) levels, and interference with copper metabolism, potentially leading to copper deficiency; short-term exposure can cause gastrointestinal distress, including nausea, vomiting, and diarrhoea (Plum et al., 2010). Environmental exposure to high levels of nickel can harm plant growth, decrease soil microbial activity, and be toxic to aquatic life. In humans, nickel primarily enters through inhalation, ingestion, and skin contact. Short-term exposure might trigger allergic reactions such as contact dermatitis, often called a nickel allergy. Long-term exposure, however, has been linked to serious health issues such as respiratory problems, lung fibrosis, and kidney damage (Das et al., 2008).

There are several general methods for the removal of heavy metals from water resources, such as chemical precipitation (Matlock et al., 2002)(Q. Wang et al., 2019)ion flotation(Hoseinian et al., 2019)(Saleem et al., 2019), ion exchange(Bashir et al., 2019) coagulation/(Sun et al., 2020)(Q. Zhang et al., 2020), adsorption (Arora, 2019), and electrochemical removal (Wu et al., 2019).Among these methods, adsorption is more advantageous due to its low cost, high efficiency and ease of operation(Tamjidi et al., 2019)(Chakraborty et al., 2022) .It is also important that the adsorbents used in the adsorption process can be reused after some of the applied cycles processes(Ince & Kaplan İnce, 2017).

Carbon black (CB) is an economical carbon-based nanomaterial featuring a high specific surface area and outstanding chemical stability(Tan Li, Wenbo Sun, Xianzhong Wang, Yan Li, Minggang Lin, Yangyi Chen, Chuyang Zhang, 2025). It

consists primarily of elemental carbon and is produced by the controlled thermal breakdown or partial combustion of hydrocarbons, yielding aggregates of carbon nanoparticles. This engineered nanomaterial differs from soot and black carbon, which originate from incomplete combustion processes (Khodabakhshi et al., 2020). In 2023, the global market for carbon black (CB) is valued at around USD 19.3 billion, equivalent to approximately 15 million metric tons, with expectations of over 66% growth over the next nine years(Rosner et al., 2024). The cost of carbon black (CB) is significantly lower, at about $1/kg, while nanotubes are priced around $600/kg(Khodabakhshi et al., 2020). Carbon black (CB) boasts remarkable electrical conductivity, excellent thermal stability characterized by a low coefficient of thermal expansion, and dependable resistance to chemicals and environmental decay. Incorporation of carbon black into polymers enhances the mechanical and thermal properties of polymers(Feng et al., 2003; Feng & Chan, 1998; B. B. Zhang et al., 2015; J. Zhang et al., 2024). Therefore, carbon black (CB) presents a strong alternative when scalability, cost, and performance converge.

Carbon blacks are mainly used as reinforcing fillers in tires and various rubber products. The incorporation of carbon black affects the properties of the compound, including its tensile strength, tear strength, modulus and abrasion resistance(Rattanasom et al., 2007)(Choi et al., 2003) . More than 92% of the worldwide production of carbon black is used in rubber manufacturing, especially in tyre production, including inner liners, sidewalls, carcasses, air springs, belts, conveyor wheels and some vibration isolation devices, (International Carbon Black Association, 2016, 2024). Metalated carbon black is a distinct variant of carbon black that has been altered by the addition of metal atoms or ions either on its surface or integrated into its structure. This alteration improves the natural properties of carbon black, including its conductivity, surface area, and catalytic activity, thereby making it suitable for advanced applications across various industries.

Metalated carbon black has become increasingly important as a multifunctional material because metal or metal-oxide modifications significantly improve its catalytic, electrochemical, adsorption, and conductivity properties. Research indicates that Fe– and N–doped carbon black composites display high oxygen reduction reaction (ORR) activity, highlighting their promising role in fuel-cell electrocatalysis. Additionally, interactions between metals and oxides have been shown to enhance both catalytic stability and activity in energy conversion systems (F. Wang et al., 2024). In environmental catalysis, Research indicates that Fe– and N–doped carbon black composites display high oxygen reduction reaction (ORR) activity, highlighting their promising role in fuel-cell electrocatalysis. Additionally, interactions between metals and oxides have been shown to enhance both catalytic stability and activity in energy conversion systems. Fe-loaded carbon supports effectively enhance CO_2 hydrogenation and pollutant elimination(Chen et al., 2024) (Schultheis et al., 2023). Nickel nanoparticles supported on carbon black can serve as catalysts for the hydrogenation of nitrophenols(Xia et al., 2016). Nitrogen doped carbon black supported on nickel nanoparticles can be employed for the hydrodeoxygenation of vanillin (Nie et al., 2017). Ni-Pd supported on carbon black, used as the catalyst for Suzuki-Miyaura coupling.(Xia et al., 2017)Ni-Pd supported on carbon black, used as the catalyst for Suzuki-Miyaura coupling; Zn-an alloy catalyst supported on carbon black can be utilised for steam reforming of methanol. Lead carbon black composites can be used as an additive in lead-ion batteries (Hu et al., 2021). These collective findings highlight metalated carbon black as a highly adaptable platform for advanced catalytic systems, energy-storage technologies, environmental remediation, conductive composites, and sensor applications.

This research involves the adsorption of heavy metal pollutants onto turmeric spent and its subsequent conversion to metalated carbon black by thermal carbonization and its characterization

2.MATERIAL AND METHODS

Materials used

Turmeric spent was sourced from Synthite Industries Pvt. Ltd. in Angamaly, Kerala, India, a reputable oleoresin extraction company. Analytical grade chemicals, including lead nitrate (Merck, Germany), zinc sulphate (Nice Chemicals, Kerala, India), nickel sulphate (Isochem, Kerala, India), ferric alum sulphate (Isochem, Kerala, India), and others, were used in the analysis. Bioadsorption of iron from the naturally occurring water bodies (red residue water, Wayanad (11.6994° N, 76.0773° E) containing a high concentration of iron was also attempted.

Methods

Preparation of turmeric spent as a bioadsorbent

Spent turmeric was collected from Synthite Industries Pvt. Ltd., Angamaly, Kerala, India. Spent was cleaned, shade-dried, powdered, and sieved (53 micron).

Preparation of metalated carbon black

Stock solutions (500 mg/L) of lead nitrate, zinc sulphate, ferric alum sulphate, and nickel sulphate were prepared as metal ion sources, from which working solutions derived from them. Red-residue water was used directly. A specific amount of spent was added to each working solution and stirred for 2 hours. The spent was then filtered and dried post-adsorption. Spent and metal-adsorbed spent were carbonized in a muffle furnace at 700 °C for 70 minutes, and then characterized.

Characterization of carbon black

Atomic absorption spectroscopy (AAS)

Carbonized spent composition and the concentration of adsorbed metals were analyzed using AAS (AA240FS Varian) at the Soil Lab, ICAR-Indian Institute of Spices Research, Kozhikode, Kerala.

CHNS analysis

Elemental analysis was performed using a CHNS Analyzer (Elementer GmbH, model Vario ELL) at the Sophisticated Test and Instrumentation Center (STIC), Cochin University of Science and Technology (CUSAT), Kochi, Kerala, India.

Scanning electron microscope with energy dispersive X-ray spectroscopy (SEM-EDS).

Surface morphology images and information on the material composition, including the elements present in the carbon black, were analyzed using SEM-EDS (SEM EDS Joel 6390LA/OXFORD XMXN). The equipment operated at an accelerating voltage of 0.5 to 30 kV, with an EDAX resolution of 136 eV. The analysis was performed at the Sophisticated Test and Instrumentation Centre (STIC), Cochin University of Science and Technology (CUSAT), Kochi, Kerala, India.

Dynamic light scattering (DLS) and Zeta potential

Particle size analysis and zeta potential are analyzed using the instrument Particle Analyser Litesizer 500 in liquid dispersions. Samples in the range of 0.3 nm to 10 µm, with concentration limits between 0.1 mg/ml, minimum sample volumes between 12 µl, and a temperature control range between 0 and 90 °C, are measured. The zeta potential of a suspension can be measured using the electrophoresis light scattering technique, with a zeta potential range of > ±1000 mV, a minimum sample volume of

50 µL for the electrode cell, and a temperature control range of 0-90 °C. The analysis was done at Bharat Mata College, autonomous, Thrikkakara, Kerala 21.

X-ray diffraction analysis (XRD)

XRD analysis of the carbonized samples was performed using a Malvern-Panalytical powder X-ray diffractometer with Cu Kα(λ=1.5406Å) radiation at a scanning speed of 2° min-1. The analysis was carried out at the Central Sophisticated Instrumentation Facility (CSIF) at the University of Calicut, Kerala, India.

3.RESULT AND DISCUSSION

Atomic Absorption Spectroscopy

Analysis of carbon black before and after metalation of various metal ions was carried out using atomic absorption spectroscopy (AAS). Turmeric as such contains many elements such as As, Cd, Ca, Cr, Cu, Fe, Hg, Mg, Mn, Pb and Zn(Muralidharan et al., 2019). During the extraction process, it was reduced to a higher content of iron, followed by Mn, Zn, Cu and Mg(Vedashree M et al., 2016) in turmeric spent. For each metal-adsorbed sample, the concentration of the specific metal was higher than normal. It can be observed from **Table 1**.

Table 1 Quantity of metals present in each sample

SI No	Sample code	Quantity of metals present(ppm)
1	Carbonized spent (CS) (before metalation)	Cu =312.5 Mn =trace Fe =11625 Zn=812.5
2	Zinc adsorbed spent (Z_1)	Zn=27125
3	Nickel adsorbed spent (N_1)	Ni=2437.5
4	Lead adsorbed spent (L_1)	Pb=37956
5	Iron adsorbed spent (Fe_1)	Fe=51875
6	Iron adsorbed spent from red residue water (Fe_2)	Fe=19812.5

It is evident that the carbonized spent contains elements like copper, manganese, and zinc. Following adsorption, the concentration of these metals increased, confirming that each metal was adsorbed into the spent.

CHNS Analysis

The elemental composition (%) of turmeric spent (S), CS, N_1, Z_1, L_1, Fe_1, and Fe_2 was analyzed by CHNS analysis and is presented in **Table 2**. All samples were heated at 700 °C for 70 minutes in a muffle furnace under limited oxygen. The results

indicate that carbonization reduced the carbon content of the carbonized spent compared with the spent. Since spent is a cellulosic material, it undergoes thermal decomposition during pyrolysis at higher temperatures, leading to complex degradation reactions that produce low molecular weight compounds and subsequently form volatile hydrocarbon gases with even lower molecular weights, resulting in low carbon content yield(Kyotani et al., 2017). Metal adsorption increased the carbon content in the iron-adsorbed sample. This is because some metals can absorb carbon dioxide (Khdary et al., 2022)(Seo et al., 2020)(Bhaduri et al., 2015). This property can be utilized by industries for fruitful production. The waste of one industry can be utilized in many industries, and a useful product can be achieved

Table 2 CHNS analysis of different samples

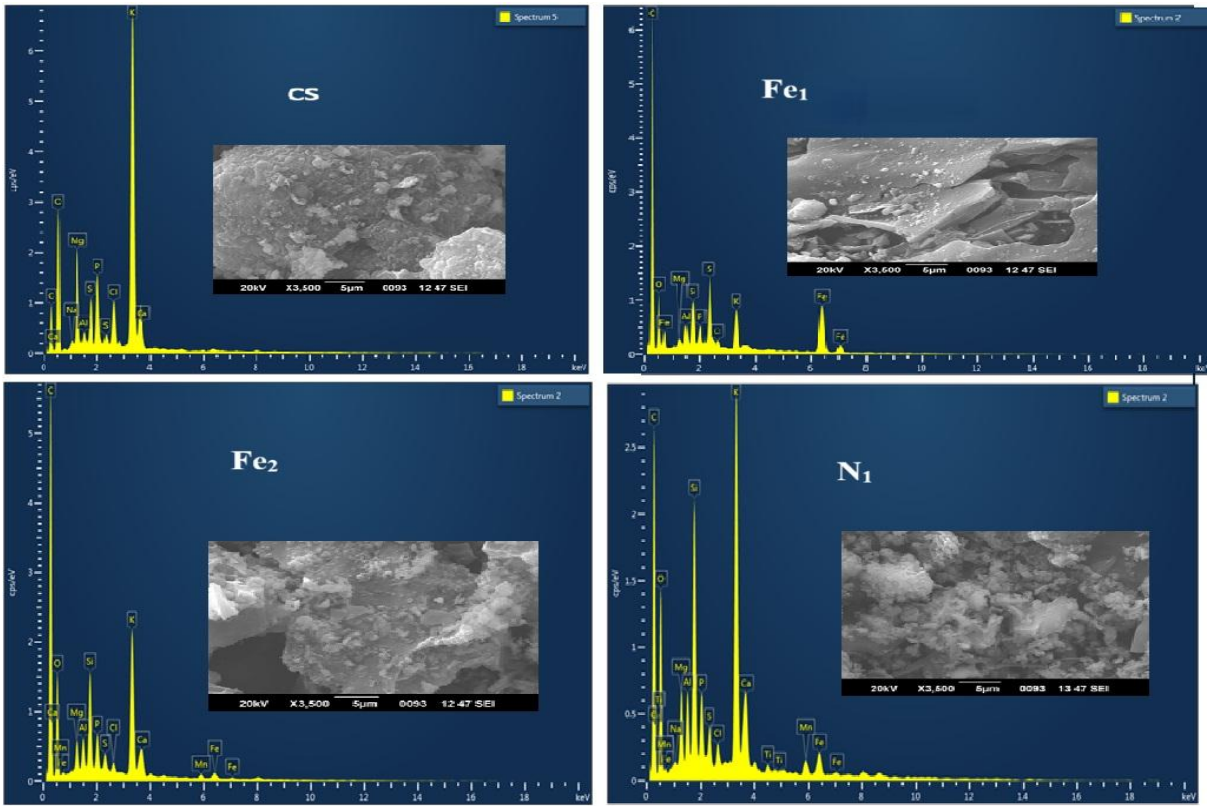
SI No	Sample Code	**N%**	**C%**	**S%**	**H%**
1	S	1.68	37.42	1.05	5.18
2	CS	0.43	9.60	2.47	1.58
3	N_1	1.16	37.31	1.43	1.62
4	Z_1	0.99	29.84	1.13	1.25
5	Fe_2	1.07	51.17	2.71	1.45
6	Fe_1	2.13	64.57	1.78	1.25
7	L_1	0.94	30.51	0.83	0.72

Scanning electron microscope with energy dispersive X-ray spectroscopy (SEM-EDS)

The energy dispersive X-ray analysis of carbon black of spent (CS) indicates the presence of C, Ca, O, Na, Mg, Al, Si, P, S, Cl, Ca and a strong peak of K. Presence of corresponding metals, iron in Fe_1 and Fe_2, Zinc in Z_1, lead in L_1 confirmed using EDS data. In the case of Ni in N_1, the presence of nickel is not evident due to the masking of the nickel peak by other elements. Nickel peaks arise around 0.5 to 1 keV,7 to 8 keV, and 8-8.5kev(Türkez et al., 2021).But the presence of nickel is confirmed from the AAS analysis. The presence of different elements is given in **Table 3.**

Table 3 Represent the presence of different elements in carbon black and metalated carbon black

CS	Fe_1	Fe_2	N_1	L_1	Z_1
C	C	C	C	C	C
Ca	Nill	Ca	Ca	Ca	Ca
O	O	O	0	O	O
Na	Nill	Nill	Na	Ca	Ca
Mg	Mg	Mg	Mg	Mg	Mg
Al	Al	Al	Al	Al	Al
Si	Si	Si	Si	Si	Si
P	P	P	P	P	P
S	S	S	S	S	S
Cl	Cl	Cl	Cl	Cl	Nill
K	K	K	K	K	K
Nill	Fe	Fe	Fe	Pb	Zn
Nill	Nill	Mn	Mn	Nill	Nill
Nill	Nill	Nill	Ti	Nill	Ti



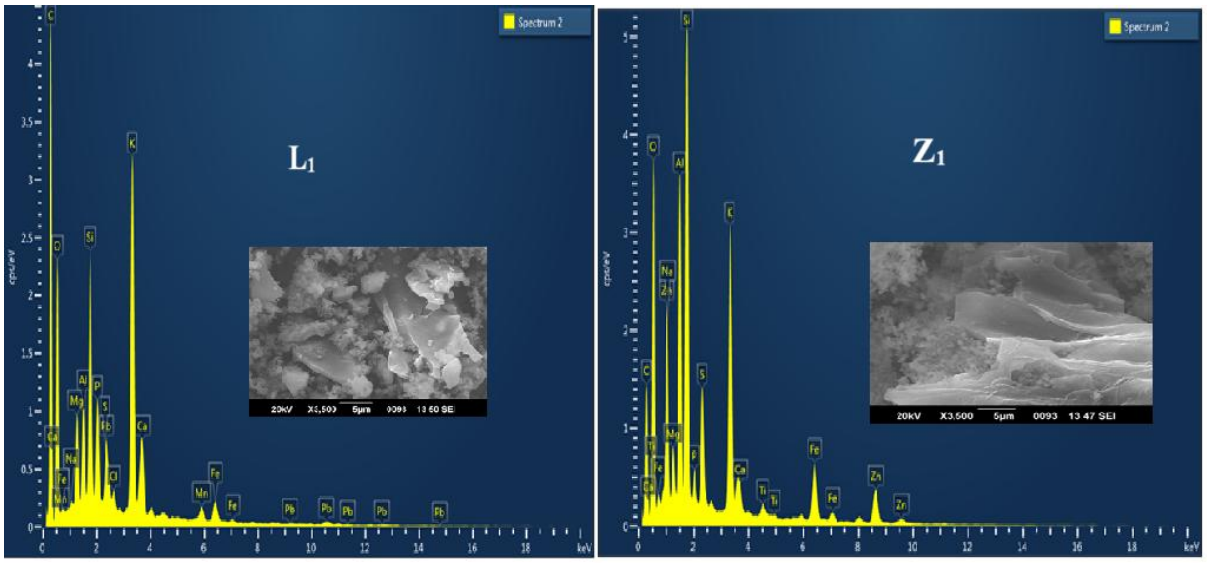


Figure.1 SEM-EDS of CS, Fe_1, Fe_2, N_1, $L_1$and Z_1

Particle size distribution

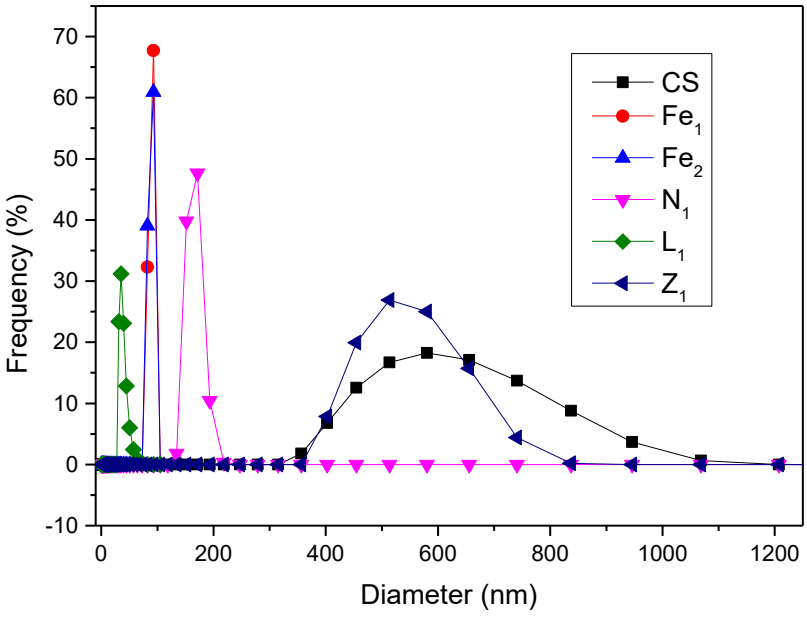


Figure.3 Particle size distribution of different samples

The particle size distributions of the different metalated samples are presented in **Figure 3**. The particle distributions of CS and Z1 occur in similar ranges, i.e., 325-1065 nm and 352-838nm, respectively. The mean peak diameter of CS is 575.2 and Z_1 at

510.7 nm respectively. Adsorption of different metals leads to a decrease in the particle size of carbon black due to enhanced dispersion and de-agglomeration of nanoparticles in aqueous medium(Chen et al., 2021). Both Fe_1 and Fe_2 show a similar particle-size distribution range, i.e., 72-101 nm. They also show a slight change in the mean peak diameter, i.e. 84.2 nm for Fe1 and 84.3 for Fe2.N1 and L1 show particle distribution in the range of 134-215 nm and maximum peak size distribution at 155.4nm and for L_1 in the range of 25-60nm and mean peak distribution at 35. 9nm.L_1 shows the lowest size. This may be due to the difference in the interaction of metals with carbon black. Peak size and standard deviation of all samples are given in **Table 4.**

Table 4 Particle size analysis of different samples

Sample code	Peak size (nm)	Peak standard deviation (nm)	Poly Dispersity Index(PI)
CS	575.2	138.1	1.271
Fe_1	84.3	4.7	2.989
Fe_2	84.8	4.9	2.793
L_1	35.9	6.5	3.055
Z_1	510.7	81.8	1.793
N_1	155.4	13.4	4.391

4.5. Zeta potential distribution

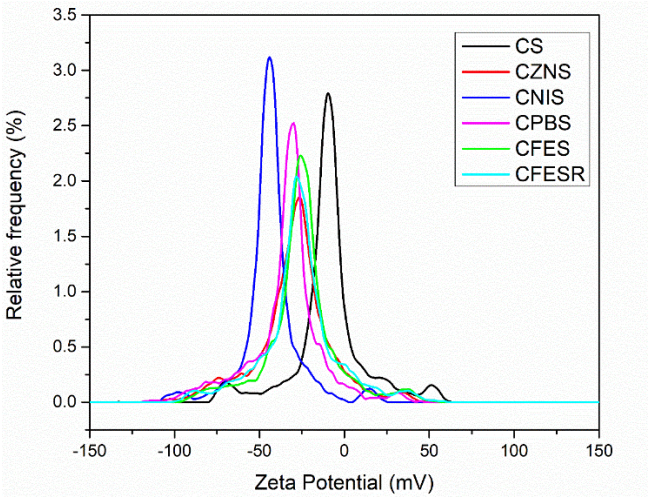


Figure.4 Zeta potential of different samples

Zeta potential provides information on colloid stability, surface charge, and surface morphology. A high positive or negative value of zeta potential indicates that there is strong repulsion between the particles and reduces the chance of agglomeration. A small zeta potential indicates a higher likelihood of agglomeration. Generally, zeta potential values greater than +30mV or

smaller than -30mV result in a stable suspension(García et al., 1997)(Yedurkar et al., 2016). The zeta potential values of all samples are compared in Figure 4. Zeta potential values of different samples are given in **Table 5**.

Table 5 Zeta potential values of different samples

Sample Code	Zeta Potential(mV)
CS	-11.9
FeS	-6.4
ZnS	-10.7
FeSR	-6.8
PbS	-4.2
NiS	-1.9

It can be seen that the zeta potential of (CS) is -11.9 mV, i.e., the surface charge of carbon black is negative as a consequence of possible dissociation of the surface oxygen-functional groups (e.g. carboxylic group) in aqueous medium(Youssry, 2018) .This negative surface charge of CS is favorable for the attraction of active pores and positively charged metal ions, resulting in electrostatic interaction(Boonamnuayvitaya et al., 2004) . A small zeta potential value shows poor stability of the suspension in aqueous media. Metal-adsorbed carbon black shows a lower zeta potential than CS. Comparing the zeta potential, the order of zeta potential is CS>Z_1>Fe_2>Fe_1>L_1>N_1. A lower negative charge indicates lower dispersion stability, leading to rapid agglomeration and preventing the formation of surface functional groups. Carbon black particles usually carry negative charge due to the deprotonated oxygen containing functional groups(Meslam et al., 2022). Decrease in the zeta potential on adsorption of positively charged metal ions is due to the charge neutralization at the surface of carbon black(Meslam et al., 2022). Here, neutralisation of COO- from COOH in carbon black with Zn^{2+}/Pb $^{2+}$. This means the formation of complexes such as -COO^{-}...Pb^{2+} /Zn $^{2+}$or -O^{-}...Pb^{2+}/Zn $^{2+}$ (COO- is from COOH and O- is from phenolic OH). Divalent and trivalent metal ions compress the double layer(Yukselen-aksoy & Kaya, 2016). Nickel-metalated carbon black useful as catalyst or catalyst support(Akamine et al., 2024). Zeta potential facilitates reactant adsorption because of less electrostatic repulsion toward charged reactants. Neutral or slightly positive surfaces attract anionic reactants important for hydrogenation and oxidation. Iron in its trivalent state gives more compression on the electrical double layer, which can also cause a decrease in zeta potential.

X-ray diffraction analysis (XRD)

CS

From the X-ray diffraction analysis of S, the peaks at 21.44 and 34.17 correspond to the diffraction planes (200) and (004), respectively [19]. These are the characteristic peaks of cellulose 1 of crystalline structure[20][21]. The XRD patterns exhibit sharp peaks at 28°, 34°, 50° and 55°. The four sharp peaks observed may indicate the presence of an unknown crystalline phase within the O-ring. The diffraction angle (2θ) of the (002) peak of crystalline graphite is known to be 26.52◦[22].

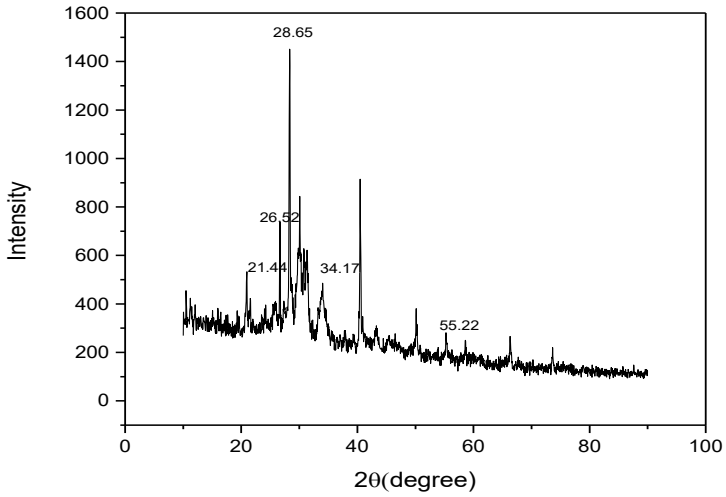


Figure.14 XRD analysis of CS

FeS

From the diffraction pattern obtained for FeS (**Figure 15)**, the 2θ values are in agreement with Fe_3O_4. The data show peaks at 2θ values 30.19,35.51,43.20,53.21,57.23 and 62.59 corresponding to the planes (220), (311), (400), (422), (511) and (440) planes of Fe_3O_4 in a cubic phase[23] .

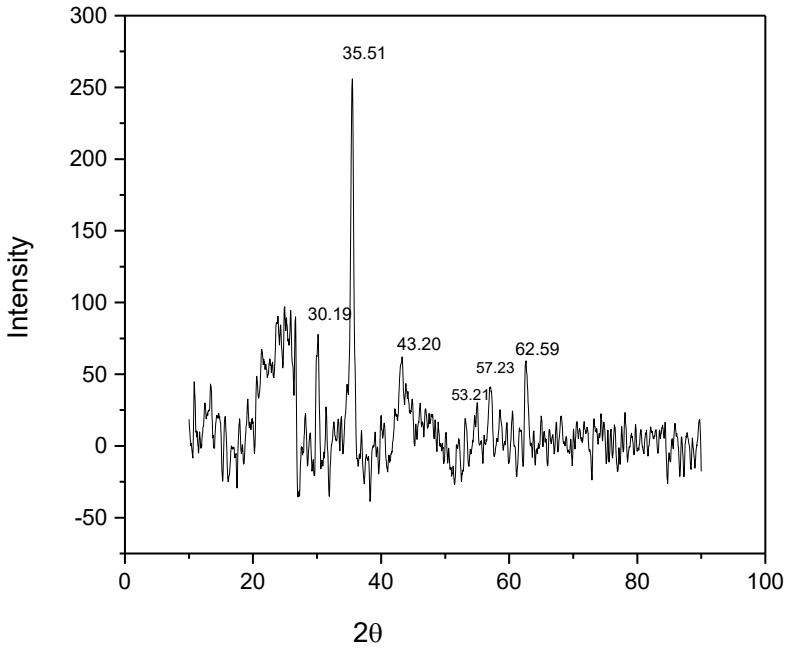


Figure.15 XRD analysis of FeS

FeSR

XRD plot of FeSR is shown in **Figure 16**. There is a slight difference in the FES peaks. The 2θ value obtained at 26.64 is assigned to the graphite (002) plane, indicating the amorphous nature of carbon black[24].Diffraction angles at 29.40,35.51,42.92,57.31 and 62.55 are in agreement with Fe_2O_3[19].

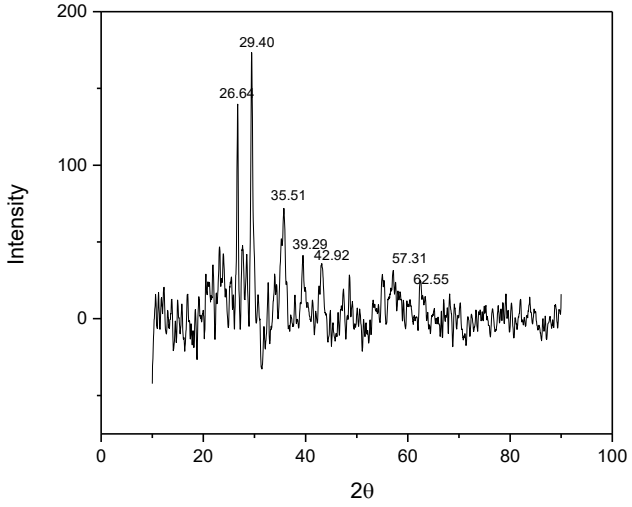


Figure.16 XRD analysis of FeSR

PbS

The XRD analysis of PbS (Figure **17)** shows peaks at 10.60,26.64,29.52,35.47,39.29,43.24 and 57.23 are peaks corresponding to lead nitrate [25].The major peaks located at 28.14,35.47 corresponding to planes (111) and (002) are characteristic peaks for the pure tetragonal alpha PbO nanoparticles[26].

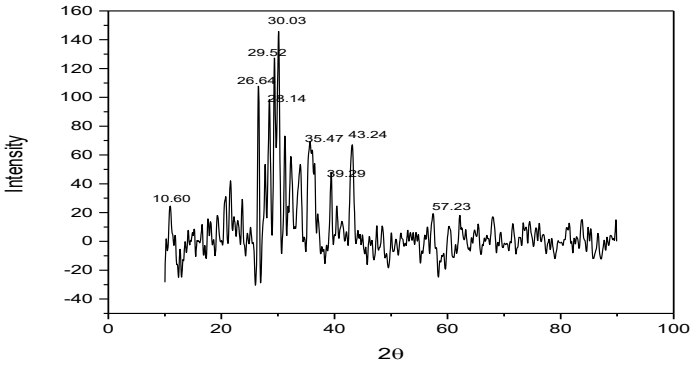


Figure.17 XRD analysis of PbS

ZnS

From the XRD studies (**Figure 18)**, the peaks obtained at 29.36,34.48,35.15,56.91 and 62.55 indicate the planes (110), (002), (101), (110), (103) and (200), respectively. These are the peaks corresponding to ZNO [27].Among these 35.15(002),39.02(100),43.24(102),62.55(110) are the characteristic peak of zinc. These planes match the HCP structure of zinc nanoparticles in the database of the Joint Committee on Powder Diffraction Standards (JCPDS Number 00-004-078[28].

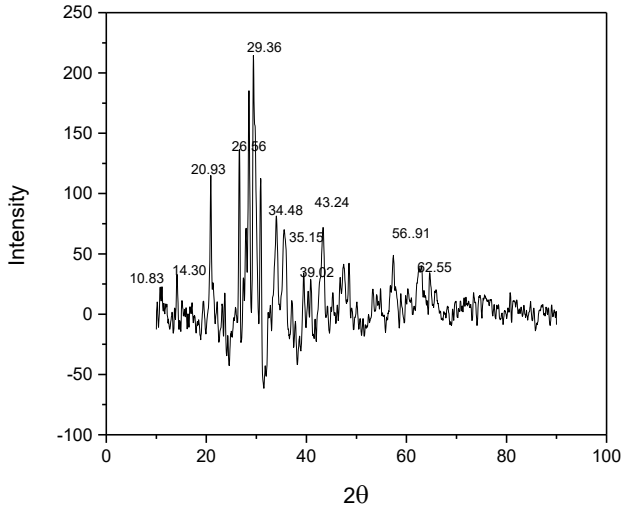


Figure.18 XRD analysis of ZnS

NiS

From the XRD pattern (**Figure 19)**, the small peaks at 45.17,52.77 are the characteristic peak of nickel refers to the JCPDS 03-1051(11). The reflections are associated with the structure of a- fcc with planes of (111),(200), suggesting single nickel nanoparticles dispersed onto the biochar surface[29], [30], [31], [32], [33].The peak at around 43 corresponds to nickel oxide[33].

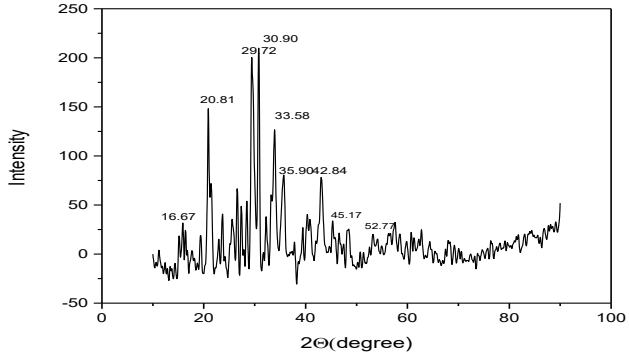


Figure.19 XRD analysis of NiS

Conclusion

In summary, turmeric spent, which is considered waste, can be used as a source of carbon black and modified into metalated carbon black. Atomic absorption spectroscopy confirmed the presence of respective metals in the metalated sample. The observed metal concentrations are as follows: Fe_1 (51875 ppm Fe), L_1 (37956 ppm Pb), Z_1 (27125 ppm Zn), and N1 (2437.5 ppm Ni). The findings show that the carbonised turmeric spent has an effective surface that can interact with and hold onto metal ions. Changes in the elemental composition during carbonization and metal treatment were analysed using CHNS analysis. Even though the carbon content was reduced during carbonization of the precursor sample, metal incorporation later increased it. SEM-EDS also confirmed the presence of Fe, Pb, and Zn, whereas Ni is masked in SEM-EDS but confirmed in AAS. DLS analysis demonstrates that metal incorporation altered particle size. The mean particle size decreased from 575.2 nm for CS to 84.3 nm for Fe_1, 84.8 nm for Fe_2, 35.9 nm for L_1,510.7 nm for Z_1, and 155.4 nm for N_1. This change or reduction in particle size suggests that metal incorporation can affect the particle aggregation and dispersion. The zeta potential value of CS (-11.9 mV) is negative and becomes further negative during metal incorporation. This indicates low colloidal stability and a greater tendency towards aggregation. XRD analysis confirmed that metal incorporation produced distinct crystalline phases. The Fe-containing sample showed the presence of Fe_3O_4 and Fe_2O_3. Whereas the Zn-containing sample showed ZnO, the Pb-containing sample showed PbO and the Ni-containing sample showed NiO, respectively. These structural changes demonstrate that the chemical nature and oxidation state of the incorporated metal strongly influence the resulting carbonaceous material.

Reference

1. Akamine, Y., Nishino, F., Yamashita, T., Tsushida, M., & Awaya, K. (2024). *The Impact of Metal − Support Interaction on the Structure and Activity of Carbon-Supported Ni Nanoparticle Catalysts for Alkaline Hydrogen Oxidation Reaction*. https://doi.org/10.1021/acsami.4c15120

2. Anbari, M. J., Tabesh, M., & Roozbahani, A. (2017). Risk assessment model to prioritize sewer pipes inspection in wastewater collection networks. *Journal of Environmental Management*, *190*, 91–101. https://doi.org/10.1016/j.jenvman.2016.12.052

3. Arora, R. (2019). Adsorption of heavy metals-a review. *Materials Today: Proceedings*, *18*, 4745–4750. https://doi.org/10.1016/j.matpr.2019.07.462

4. Bashir, A., Malik, L. A., Ahad, S., Manzoor, T., Bhat, M. A., Dar, G. N., & Pandith, A. H. (2019). Removal of heavy metal ions from aqueous system by ion-exchange and biosorption methods. *Environmental Chemistry Letters*, *17*(2), 729–754. https://doi.org/10.1007/s10311-018-00828-y

5. Bhaduri, G. A., Alamiry, M. A. H., & Šiller, L. (2015). Nickel Nanoparticles for Enhancing Carbon Capture. *Journal of Nanomaterials*, *2015*. https://doi.org/10.1155/2015/581785

6. Boonamnuayvitaya, V., Chaiya, C., & Tanthapanichakoon, W. (2004). *Removal of heavy metals by adsorbent prepared from pyrolyzed coffee residues and clay*. *35*, 11–22. https://doi.org/10.1016/S1383-5866(03)00110-2

7. Bužarovska, A., Dimitrovski, D., & Trajkovska Petkoska, A. (2025). Development of Poly(L-lactic acid) Films Containing Curcuma lunga L. Extract for Active Cheese Packaging. *Processes*, *13*(6), 1–18. https://doi.org/10.3390/pr13061881

8. Cakrawati, D., Sugiarti, Y., & Handayani, S. (2024). Effect of ragi tape fermentation on physicochemical properties, phenolic compounds, and antioxidant capacity of turmeric spent. *Maret*, *18*(1), 182–188. https://doi.org/10.21107/agrointek.v18i1.17604

9. Chakraborty, R., Asthana, A., Singh, A. K., Jain, B., & Susan, A. B. H. (2022). Adsorption of heavy metal ions by various low-cost adsorbents: a review. *International Journal of Environmental Analytical Chemistry*, *102*(2), 342–379. https://doi.org/10.1080/03067319.2020.1722811

10. Chen, Y., Chen, H., Lo, M., & Chen, Y. (2021). *Modification of Carbon Black with Hydrogen Peroxide for High Performance Anode Catalyst of Direct Methanol Fuel Cells*. 1–13.

11. Chen, Y., Jiang, L., Lin, S., Dong, P., Fu, X., Wang, Y., Liu, Q., & Wu, M. (2024). Carbon-Supported Fe-Based Catalyst for Thermal-Catalytic CO2 Hydrogenation into C2+ Alcohols: The Effect of Carbon Support Porosity on Catalytic Performance. *Molecules*, *29*(19). https://doi.org/10.3390/molecules29194628

12. Choi, S. S., Nah, C., & Jo, B. W. (2003). Properties of natural rubber composites reinforced with silica or carbon black: Influence of cure accelerator content and filler dispersion. *Polymer International*, *52*(8), 1382–1389. https://doi.org/10.1002/pi.1232

13. Das, K. K., Das, S. N., & Dhundasi, S. A. (2008). Nickel, its adverse health effects & oxidative stress. *Indian Journal of Medical Research*, *128*(4), 412–425.

14. Dasharathy, S., Arjunan, S., Maliyur Basavaraju, A., Murugasen, V., Ramachandran, S., Keshav, R., & Murugan, R. (2022). Mutagenic, Carcinogenic, and Teratogenic Effect of Heavy Metals. *Evidence-Based Complementary and Alternative Medicine*, *2022*. https://doi.org/10.1155/2022/8011953

15. Feng, J., & Chan, C. M. (1998). Carbon black-filled immiscible blends of poly(vinylidene fluoride) and high density polyethylene: Electrical properties and morphology. *Polymer Engineering and Science*, *38*(10), 1649–1657. https://doi.org/10.1002/pen.10335

16. Feng, J., Chan, C. M., & Li, J. X. (2003). A Method to Control the Dispersion of Carbon Black in an Immiscible Polymer Blend. *Polymer Engineering and Science*, *43*(5), 1058–1063. https://doi.org/10.1002/pen.10089

17. García, A. B., Cuesta, A., Montes-Morán, M. A., Martínez-Alonso, A., & Tascón, J. M. D. (1997). Zeta potential as a tool to characterize plasma oxidation of carbon fibers. *Journal of Colloid and Interface Science*, *192*(2), 363–367. https://doi.org/10.1006/jcis.1997.5007

18. Goel, A., Kunnumakkara, A. B., & Aggarwal, B. B. (2008). Curcumin as “Curecumin”: From kitchen to clinic. *Biochemical Pharmacology*, *75*(4), 787–809. https://doi.org/10.1016/j.bcp.2007.08.016

19. Hamdy, A., Mostafa, M. K., & Nasr, M. (2019). Techno-economic estimation of electroplating wastewater treatment using zero-valent iron nanoparticles: batch optimization, continuous feed, and scaling up studies. *Environmental Science and Pollution Research*, *26*(24), 25372–25385. https://doi.org/10.1007/s11356-019-05850-3

20. Hashim, K. S., Shaw, A., Al Khaddar, R., Pedrola, M. O., & Phipps, D. (2017). Iron removal, energy consumption and operating cost of electrocoagulation of drinking water using a new flow column reactor. *Journal of Environmental Management*, *189*, 98–108. https://doi.org/10.1016/j.jenvman.2016.12.035

21. Hoseinian, F. S., Rezai, B., Kowsari, E., & Safari, M. (2019). A hybrid neural network/genetic algorithm to predict

Zn(II) removal by ion flotation. *Separation Science and Technology (Philadelphia)*, *55*(6), 1197–1206. https://doi.org/10.1080/01496395.2019.1582543

22. Hu, C., Li, J., Li, Q., Lan, T., Zhang, J., Zhou, S., Rao, Y., & Cao, J. (2021). Rapid preparation of nano lead sulfate-lead carbon black composite by microwave method as a negative electrode additive for lead-carbon batteries. *Electrochimica Acta*, *384*, 138411. https://doi.org/10.1016/j.electacta.2021.138411

23. Ince, M., & Kaplan İnce, O. (2017). An Overview of Adsorption Technique for Heavy Metal Removal from Water/Wastewater: A Critical Review. *International Journal of Pure and Applied Sciences*, *3*(2), 10–19. https://doi.org/10.29132/ijpas.358199

24. International Carbon Black Association. (2016). Carbon Black User ' s Guide. *Carbon Black User's Guide*, 36. http://www.carbon-black.org/images/docs/2016-ICBA-Carbon-Black-User-Guide.pdf

25. International Carbon Black Association. (2024). *Carbon Black User's Guide: Safety, Health, & Environmental Information*. *September*, 36.

26. Joshi, P., Joshi, S., Semwal, D. K., Bisht, A., Sharma, S., & Dwivedi, J. (2021). Chemical composition, antioxidative and antimicrobial activities of turmeric spent oleoresin. *Industrial Crops and Products*, *162*(September 2020), 113278. https://doi.org/10.1016/j.indcrop.2021.113278

27. Kanagaraj, B., Anand, N., Raj R, S., & Lubloy, E. (2024). Utilizing agricultural turmeric bulbs as an alternative to traditional coarse aggregates in geopolymer concrete to explore its engineering properties. *Developments in the Built Environment*, *17*(January), 100358. https://doi.org/10.1016/j.dibe.2024.100358

28. Karim, A., Raji, Z., Karam, A., & Khalloufi, S. (2023). Valorization of Fibrous Plant-Based Food Waste as Biosorbents for Remediation of Heavy Metals from Wastewater—A Review. *Molecules*, *28*(10), 1–21. https://doi.org/10.3390/molecules28104205

29. Kerur, S. S., Bandekar, S., Hanagadakar, M. S., Nandi, S. S., Ratnamala, G. M., & Hegde, P. G. (2020). Removal of hexavalent Chromium-Industry treated water and Wastewater: A review. *Materials Today: Proceedings*, *42*, 1112–1121. https://doi.org/10.1016/j.matpr.2020.12.492

30. Khatri, N., Tyagi, S., & Rawtani, D. (2017). Recent strategies for the removal of iron from water : A review. *Journal of Water Process Engineering*, *19*(13), 291–304. https://doi.org/10.1016/j.jwpe.2017.08.015

31. Khdary, N. H., Alayyar, A. S., Alsarhan, L. M., Alshihri, S., & Mokhtar, M. (2022). Metal Oxides as Catalyst/Supporter for CO2 Capture and Conversion, Review. *Catalysts*, *12*(3). https://doi.org/10.3390/catal12030300

32. Khodabakhshi, S., Fulvio, P. F., & Andreoli, E. (2020). Carbon black reborn: Structure and chemistry for renewable energy harnessing. *Carbon*, *162*, 604–649. https://doi.org/10.1016/j.carbon.2020.02.058

33. Klaudia Jomova , Suliman Y Alomar , Eugenie Nepovimova , Kamil Kuca, M. V. (2025). Heavy metals: toxicity and human health effects. *Arch Toxicol*, *99*(9), 153–209. https://doi.org/10.1007/s00204-024-03903-2.

34. Kyotani, M., Hiratani, K., Okada, T., & Matsushita, S. (2017). *Preparation of 2D Carbon Materials by Chemical Carbonization of Cellulosic Materials to Avoid Thermal Decomposition*. *1700061*. https://doi.org/10.1002/gch2.201700061

35. Landim Neves, M. I., Strieder, M. M., Vardanega, R., Silva, E. K., & Meireles, M. A. A. (2020). Biorefinery of

turmeric (: Curcuma longa L.) using non-thermal and clean emerging technologies: An update on the curcumin recovery step. *RSC Advances*, *10*(1), 112–121. https://doi.org/10.1039/c9ra08265d

36. Lu, H., & Yu, S. (2018). Spatio-temporal variational characteristics analysis of heavy metals pollution in water of the typical northern rivers, China. *Journal of Hydrology*, *559*, 787–793. https://doi.org/10.1016/j.jhydrol.2018.02.081

37. Luo, P., Mu, Y., Wang, S. et al. (2022). Exploring sustainable solutions for the water environment in Chinese and Southeast Asian cities. *Ambio*, *51*, 1199–1218. https://doi.org/https://doi.org/10.1007/s13280-021-01654-3

38. Luo, P., Liu, L., Wang, S., Ren, B., He, B., & Nover, D. (2022). Influence assessment of new Inner Tube Porous Brick with absorbent concrete on urban floods control. *Case Studies in Construction Materials*, *17*(June), e01236. https://doi.org/10.1016/j.cscm.2022.e01236

39. Matlock, M. M., Howerton, B. S., & Atwood, D. A. (2002). Chemical precipitation of heavy metals from acid mine drainage. *Water Research*, *36*(19), 4757–4764. https://doi.org/10.1016/S0043-1354(02)00149-5

40. Meslam, M., Elzatahry, A. A., & Youssry, M. (2022). Promising aqueous dispersions of carbon black for semisolid flow battery application. *Colloids and Surfaces A: Physicochemical and Engineering Aspects*, *648*(May), 129376. https://doi.org/10.1016/j.colsurfa.2022.129376

41. Mu, D., Luo, P., Lyu, J., Zhou, M., Huo, A., Duan, W., Nover, D., He, B., & Zhao, X. (2021). Impact of temporal rainfall patterns on flash floods in Hue City, Vietnam. *Journal of Flood Risk Management*, *14*(1), 1–15. https://doi.org/10.1111/jfr3.12668

42. Muralidharan, L., Gaur, S., & Chinmay, M. (2019). Analysis of Heavy and Trace Metals in Golden Ingredient Turmeric (Curcuma longa) of Mumbai, Maharashtra. *International Journal of Bio-Science and Bio-Technology (IJBSBT)*, *11*(8), 4–9. https://doi.org/10.13140/RG.2.2.25945.88168

43. Nagarajan, S., Kubra, I. R., & Rao, L. J. M. (2010). Separation of Curcuminoids Enriched Fraction from Spent Turmeric Oleoresin and Its Antioxidant Potential. *Journal of Food Science*, *75*(6), 158–162. https://doi.org/10.1111/j.1750-3841.2010.01696.x

44. Nampoothiri, S. V., Lekshmi, P. C., Venugopalan, V. V., & Menon, A. N. (2012). Antidiabetic and antioxidant potentials of spent turmeric oleoresin, a by-product from curcumin production industry. *Asian Pacific Journal of Tropical Disease*, *2*(SUPPL.1), S169–S172. https://doi.org/10.1016/S2222-1808(12)60146-7

45. Narayan Thorat, B., & Kumar Sonwani, R. (2022). Current technologies and future perspectives for the treatment of complex petroleum refinery wastewater: A review. *Bioresource Technology*, *355*(February), 127263. https://doi.org/10.1016/j.biortech.2022.127263

46. Nie, R., Yang, H., Zhang, H., Yu, X., Lu, X., Zhou, D., & Xia, Q. (2017). Mild-temperature hydrodeoxygenation of vanillin over porous nitrogen-doped carbon black supported nickel nanoparticles. *Green Chemistry*, *19*(13), 3126–3134. https://doi.org/10.1039/c7gc00531h

47. Nur-E-Alam, M., Mia, M. A. S., Ahmad, F., & Rahman, M. M. (2020). An overview of chromium removal techniques from tannery effluent. *Applied Water Science*, *10*(9), 1–22. https://doi.org/10.1007/s13201-020-01286-0

48. Plum, L. M., Rink, L., & Hajo, H. (2010). The essential toxin: Impact of zinc on human health. *International Journal of Environmental Research and Public Health*, *7*(4), 1342–1365. https://doi.org/10.3390/ijerph7041342

49. Qasem, N. A. A., Mohammed, R. H., & Lawal, D. U. (2021). Removal of heavy metal ions from wastewater: a comprehensive and critical review. *Npj Clean Water*, *4*(1). https://doi.org/10.1038/s41545-021-00127-0

50. Raj, K., & Das, A. P. (2023). Lead pollution: Impact on environment and human health and approach for a sustainable solution. *Environmental Chemistry and Ecotoxicology*, *5*(February), 79–85. https://doi.org/10.1016/j.enceco.2023.02.001

51. Rattanasom, N., Saowapark, T., & Deeprasertkul, C. (2007). Reinforcement of natural rubber with silica/carbon black hybrid filler. *Polymer Testing*, *26*(3), 369–377. https://doi.org/10.1016/j.polymertesting.2006.12.003

52. Rosner, F., Bhagde, T., Slaughter, D. S., Zorba, V., & Stokes-Draut, J. (2024). Techno-economic and carbon dioxide emission assessment of carbon black production. *Journal of Cleaner Production*, *436*(August 2023), 140224. https://doi.org/10.1016/j.jclepro.2023.140224

53. Saleem, H., Pal, P., Haija, M. A., & Banat, F. (2019). Regeneration and reuse of bio-surfactant to produce colloidal gas aphrons for heavy metal ions removal using single and multistage cascade flotation. *Journal of Cleaner Production*, *217*(2019), 493–502. https://doi.org/10.1016/j.jclepro.2019.01.216

54. Schultheis, S. E., Herold, F., Koh, E. S., Oefner, N., Hungsberg, M., Drochner, A., & Etzold, B. J. M. (2023). Iron supported on beaded carbon black as active, selective and stable catalyst for direct CO2 to olefin conversion. *Catalysis Communications*, *175*(February), 106622. https://doi.org/10.1016/j.catcom.2023.106622

55. Seo, S., Lages, B., & Kim, M. (2020). Catalytic CO2 absorption in an amine solvent using nickel nanoparticles for post-combustion carbon capture. *Journal of CO2 Utilization*, *36*(October 2019), 244–252. https://doi.org/10.1016/j.jcou.2019.11.011

56. Shahabi Nejad, M., & Sheibani, H. (2022). Super-efficient removal of arsenic and mercury ions from wastewater by nanoporous biochar-supported poly 2-aminothiophenol. *Journal of Environmental Chemical Engineering*, *10*(3), 107363. https://doi.org/10.1016/J.JECE.2022.107363

57. Shambu, B. S., Rajeshwari, K. M., Bindya, S., Hemavathi, A. B., Keerthi, M. L., Lakshmi, S., Singh, P., Shivamallu, C., Abass, K. S., Stupin, V., Silina, E., & Kollur, S. P. (2026). Turmeric essential oil infused pectin blended sodium alginate polymer as sustainable food packaging material. *Scientific Reports*, *16*(1), 1–15. https://doi.org/10.1038/s41598-026-38254-8

58. Sharma, P., Iqbal, H. M. N., & Chandra, R. (2022). Evaluation of pollution parameters and toxic elements in wastewater of pulp and paper industries in India: A case study. *Case Studies in Chemical and Environmental Engineering*, *5*(September 2021), 100163. https://doi.org/10.1016/j.cscee.2021.100163

59. Slaček, G., Kotnik, P., Osmić, A., Postružnik, V., Knez, Ž., Finšgar, M., & Knez Marevci, M. (2023). The Extraction Process, Separation, and Identification of Curcuminoids from Turmeric Curcuma longa. *Foods*, *12*(21). https://doi.org/10.3390/foods12214000

60. Staszak, K., & Wieszczycka, K. (2023). Recovery of Metals from Wastewater—State-of-the-Art Solutions with the Support of Membrane Technology. *Membranes*, *13*(1). https://doi.org/10.3390/membranes13010114

61. Sun, Y., Zhou, S., Pan, S. Y., Zhu, S., Yu, Y., & Zheng, H. (2020). Performance evaluation and optimization of flocculation process for removing heavy metal. *Chemical Engineering Journal*, *385*(December 2019), 123911. https://doi.org/10.1016/j.cej.2019.123911

62. Syed, M. A., Siddaramaiah, Syed, R. T., & Syed, A. A. (2010). Investigation on physico-mechanical properties, water, thermal and chemical ageing of unsaturated polyester/turmeric spent composites. *Polymer - Plastics Technology and Engineering*, *49*(6), 555–559. https://doi.org/10.1080/03602550903533974

63. Tamjidi, S., Esmaeili, H., & Kamyab Moghadas, B. (2019). Application of magnetic adsorbents for removal of heavy metals from wastewater: A review study. *Materials Research Express*, *6*(10). https://doi.org/10.1088/2053-1591/ab3ffb

64. Tan Li, Wenbo Sun, Xianzhong Wang, Yan Li, Minggang Lin, Yangyi Chen, Chuyang Zhang, H. Q. (2025). Carbon black and polyetherimide modified ES nonwovens for low-cost and continuous seawater desalination. *Separation and Purification Technology, 354*(3), 128939. https://doi.org/https://doi.org/10.1016/j.seppur.2024.128939.

65. Tripathy, Banismita, Akankshya, A. P. (2024). Detection of Environmental Microfiber Pollutants through Vibrational Spectroscopic Techniques: Recent Advances of Environmental Monitoring and Future Prospects. *Critical Reviews in Analytical Chemistry*, *54*(7), 1925–1935. https://doi.org/https://doi.org/10.1080/10408347.2022.2144994

66. Türkez, H., Arslan, M. E., Sönmez, E., Tatar, A., Geyikoğlu, F., Açikyildiz, M., & Mardinoğlu, A. (2021). Safety Assessments of Nickel Boride Nanoparticles on the Human Pulmonary Alveolar Cells by Using Cell Viability and Gene Expression Analyses. *Biological Trace Element Research*, *199*(7), 2602–2611. https://doi.org/10.1007/s12011-020-02374-7

67. Vedashree M, Pradeep K, Ravi R, & Madhava Naidu M. (2016). *Turmeric Spent Flour: Value Addition to Breakfast Food*. *1*(2), 1002–1006. www.austinpublishinggroup.com

68. Wang, F., Zheng, Z., Wu, D., Wan, H., Chen, G., Zhang, N., Liu, X., & Ma, R. (2024). Tunable Pt-NiO interaction-induced efficient electrocatalytic water oxidation and methanol oxidation. *Chemical Science*, *15*(26), 10172–10181. https://doi.org/10.1039/d4sc00454j

69. Wang, Q., Yu, J., Chen, X. Y., Du, D., Wu, R., Qu, G., Guo, X., Jia, H., & Wang, T. (2019). Non-thermal plasma oxidation of Cu(II)-EDTA and simultaneous Cu(II) elimination by chemical precipitation. *Journal of Environmental Management*, *248*(June), 109237. https://doi.org/10.1016/j.jenvman.2019.07.008

70. Wang, R., Shu, J., Chen, M., Wang, R., He, D., Wang, J., Tang, C., Han, Y., & Luo, Z. (2021). An innovative method for fractionally removing high concentrations of Ni2+, PO43−, TP, COD, and NH4+-N from printed-circuit-board nickel plating wastewater. *Separation and Purification Technology*, *260*(August 2020), 118241. https://doi.org/10.1016/j.seppur.2020.118241

71. Wang, Z., Luo, P., Zha, X., Xu, C., Kang, S., Zhou, M., Nover, D., & Wang, Y. (2022). Overview assessment of risk evaluation and treatment technologies for heavy metal pollution of water and soil. *Journal of Cleaner Production*, *379*, 134043. https://doi.org/10.1016/J.JCLEPRO.2022.134043

72. Wei, W., Ma, R., Sun, Z., Zhou, A., Bu, J., Long, X., & Liu, Y. (2018). Effects of mining activities on the release of heavy metals (HMs) in a typical mountain headwater region, the Qinghai-Tibet Plateau in China. *International Journal of Environmental Research and Public Health*, *15*(9). https://doi.org/10.3390/ijerph15091987

73. World Health Organization. (2004). *Guidelines for Drinking Water Quality:Recommendations* (3rd ed.). World Health Organization.

74. Wu, T., Liu, C., Kong, B., Sun, J., Gong, Y., Liu, K., Xie, J., Pei, A., & Cui, Y. (2019). Amidoxime-Functionalized

Macroporous Carbon Self-Refreshed Electrode Materials for Rapid and High-Capacity Removal of Heavy Metal from Water. *ACS Central Science*, *5*(4), 719–726. https://doi.org/10.1021/acscentsci.9b00130

75. Xia, J., Fu, Y., He, G., Sun, X., & Wang, X. (2017). Core-shell-like Ni-Pd nanoparticles supported on carbon black as a magnetically separable catalyst for green Suzuki-Miyaura coupling reactions. *Applied Catalysis B: Environmental*, *200*, 39–46. https://doi.org/10.1016/j.apcatb.2016.06.066

76. Xia, J., He, G., Zhang, L., Sun, X., & Wang, X. (2016). Hydrogenation of nitrophenols catalyzed by carbon black-supported nickel nanoparticles under mild conditions. *Applied Catalysis B: Environmental*, *180*, 408–415. https://doi.org/10.1016/j.apcatb.2015.06.043

77. Yedurkar, S., Maurya, C., & Mahanwar, P. (2016). Biosynthesis of Zinc Oxide Nanoparticles Using Ixora Coccinea Leaf Extract—A Green Approach. *Open Journal of Synthesis Theory and Applications*, *05*(01), 1–14. https://doi.org/10.4236/ojsta.2016.51001

78. Youssry, M. (2018). Aqueous dispersions of carbon black and its hybrid with carbon nano fibers. *RSC Advances*, *8*, 32119–32131. https://doi.org/10.1039/c8ra05446k

79. Yukselen-aksoy, Y., & Kaya, A. (2016). *The Zeta Potential of a Mixed Mineral Clay in the Presence of Cations*. *1*(1), 14–21.

80. Zha, X., Luo, P., Zhu, W., Wang, S., Lyu, J., Zhou, M., Huo, A., & Wang, Z. (2021). A bibliometric analysis of the research on Sponge City: Current situation and future development direction. *Ecohydrology*, *14*(7), 1–16. https://doi.org/10.1002/eco.2328

81. Zhang, B. B., Chen, Y., Wang, F., & Hong, R. Y. (2015). Surface modification of carbon black for the reinforcement of polycarbonate/acrylonitrile-butadiene-styrene blends. *Applied Surface Science*, *351*, 280–288. https://doi.org/10.1016/j.apsusc.2015.05.106

82. Zhang, J., Li, J., Li, H., Yang, M., Li, Y., Qi, Y., Xu, Y., Hu, W., & Liu, B. (2024). Recent Overview and Future Research Prospects of Cross-linked Polyethylene Materials: Cross-linking Methods and Applications. *Preprints*. https://doi.org/10.20944/preprints202409.1601.v1

83. Zhang, Q., Ye, X., Li, H., Chen, D., Xiao, W., Zhao, S., Xiong, R., & Li, J. (2020). Cumulative effects of pyrolysis temperature and process on properties, chemical speciation, and environmental risks of heavy metals in magnetic biochar derived from coagulation-flocculation sludge of swine wastewater. *Journal of Environmental Chemical Engineering*, *8*(6), 104472. https://doi.org/10.1016/j.jece.2020.104472

84. Zhu, W., Wang, S., Luo, P., Zha, X., Cao, Z., Lyu, J., Zhou, M., He, B., & Nover, D. (2022). A Quantitative Analysis of the Influence of Temperature Change on the Extreme Precipitation. *Atmosphere*, *13*(4), 1–15. https://doi.org/10.3390/atmos13040612